Power Engineering and Engineering Thermophysics
https://www.acadlore.com/journals/PEET

Efficiency Optimization in Solar Water Heaters: A Comparative CFD Study of Design Configurations

Zvawanda Paul[1,2*], Peace-Maker Masukume[2]

[1] Chemical Engineering Discipline, University of KwaZulu-Natal, 4000 Durban, South Africa
[2] Department of Fuels and Energy Engineering, Midlands State University, ZW170407 Gweru, Zimbabwe

[*] Correspondence: Zvawanda Paul (zvawandap@staff.msu.ac.zw)

Received: 10-28-2023 **Revised:** 12-02-2023 **Accepted:** 12-10-2023

Citation: Z. Paul and P. M. Masukume, "Efficiency optimization in solar water heaters: A comparative CFD study of design configurations," *Power Eng. Eng. Thermophys.*, vol. 2, no. 4, pp. 238–249, 2023. https://doi.org/10.56578/peet020405.

Abstract: In the realm of renewable energy, the optimization of solar water heating (SWH) systems stands paramount for addressing the escalating energy demands. This investigation delves into the pivotal role of design configurations in augmenting the efficiency of SWH systems, with a focus on diverse climatic and locational contexts. Employing the k-omega turbulence model within the ANSYS software framework, a meticulous evaluation of three distinct design configurations, namely, tube-over-plate, tube-under-plate, and tube-in-line-with-plate, is presented. The essence of this study lies not merely in delineating the intrinsic characteristics of these configurations but in a comparative assessment of their efficiencies to ascertain the most efficacious design for superior SWH performance. The adoption of the k-omega turbulence model is instrumental in capturing the intricate fluid dynamics that significantly influence SWH efficiency. The findings reveal that the tube-under-plate configuration exhibits remarkable efficiency, while the tube-in-line-with-plate arrangement demonstrates comparably effective performance. These insights represent a substantial contribution to the advancement of water heating technology, paving the way for more effective and sustainable energy solutions.

Keywords: Solar water heaters; Thermal characteristics; k-omega; Computational fluid dynamics; ANSYS software; Temperature; Solar heat collection

1 Introduction

Solar water heaters, integral components of solar energy systems, stand as a pivotal solution in the realm of renewable energy. Harnessing solar radiation, these systems provide a cost-effective and practical means for hot water supply, particularly in residential settings. Recognized for their economic viability, solar water heaters are versatile, catering to a diverse range of applications including residential homes, community centers, hospitality sectors, and industrial settings. Common features across various designs of solar water heaters include solar collectors for energy capture, insulated storage tanks to maintain temperature consistency, and essential structural components like connecting pipes and instrumentation. This study delves into the efficiency optimization of SWH systems. The primary aim is to enhance their operational efficiency and broaden the scope of utilization. Beyond conventional approaches to SWH, this research seeks to redefine system functionality, merging a focused approach with sustainable energy solutions. The exploration of integrated solar water-heating systems aims to push the boundaries of efficiency and environmental responsibility. In the quest to advance solar hydrothermal technology, significant contributions have emerged from various studies. Notably, the work of Seretse et al. [1] focused on improving heat transfer efficiency from the working fluid to the absorption wall of the pipe. Techniques such as increasing the contact area between the fluid and absorbing pipe or introducing flow obstacles have been investigated to enhance heat transfer rates. These methods are pivotal in moderating fluid velocity, reducing pipe stress, and prolonging fluid residence time, thus optimizing the thermal performance of solar water heaters. This study primarily focused on assessing the impact of thermal conductivity in drain pipes with various micro-profiles. The findings were juxtaposed against results obtained from an adsorbent pipe without fine particles, facilitating a comprehensive understanding of the influence of micro-profiles on thermal behavior.

Prakash [2] embarked on the development of an innovative solar hot water system aimed at reducing energy consumption and minimizing heat loss in buildings. Their approach included the integration of suitable roof insulation, coupled with the utilization of commercially available computerized humidifiers in an isolated advanced roofing system, inclusive of solar humidifiers. This study critically analyzed the factors affecting the efficiency and insulation properties of SWH systems. Additionally, it established an optimized approach for high-rise roofing, informed by the results. In winter conditions, the advanced roofing system achieved a notable increase in temperature, reaching up to 60°C, while concurrently producing approximately 25 liters of hot water per day. Conversely, during summer, the technology effectively regulated roof temperature to around 27°C. Another significant contribution came from Sadhishkumar and Balusamy [3], who investigated the application of phase change materials (PCMs) for the storage of solar energy, subsequently using this stored energy for nocturnal water heating in residential settings. The study employed three distinct methodologies to evaluate the efficiency of glass solar water heaters: operating without a reflector, with a reflector, and with a reflector combined with PCM, specifically paraffin wax. This thorough analysis was aimed at understanding the various factors influencing the operational efficiency of water-in-glass evacuated tube solar receiver pipes. Alongside presenting the results of a numerical analysis on water flow within these pipes, the study correlated these findings with simulation results. It was suggested that the implementation of the recommended configurations could potentially elevate the temperature of stored water by approximately 5 to 7 degrees Celsius over extended periods. Gujrathi et al. [4] conducted a study using the Ansys 15.0 Workbench to simulate a Parabolic Trough Collector (PTC). The PTC, designed with an aspect ratio of 25, underwent a series of simulations involving four distinct mass flow rates: 0.25 kg/hr, 0.5 kg/hr, 0.75 kg/hr, and 1 kg/hr. The study presented findings on the PTC's performance, focusing on the heat transfer characteristics such as thermal flux, Nusselt number, and heat transfer coefficient across various mass flow rates. At a mass flow rate of 0.25 kg/hr and a collector efficiency of 51.2%, the maximum water temperature was determined to be 3670 K. Interestingly, it was observed that increasing the mass flow rate from 0.25 kg/hr to 1 kg/hr led to a decrease in water temperature from 3660 K to 3180 K, with the highest exit water temperature being 3660 K. This inverse relationship between the mass flow rate and temperature was further supported by an increase in the heat transfer rate, as evidenced by higher Nusselt numbers and an enhanced heat transfer ratio.

Raj et al. [5] aimed to evaluate the performance of flat table solar water-heater riser pipes, both with and without the inclusion of particles. Their research extended to riser pipes with varied contact areas, encompassing designs such as modified fine inverted riser tubes, fine riser tubes with a 270° contact area, standard fine riser tubes with a 90° contact area, and standard fine reversed riser tubes. Each variant underwent thorough examination. The study highlighted a direct correlation between the thermal conductivity of fins and their surface area. By examining five different propeller types, an increase in the contact area between the riser pipe and micro heat transfer elements was achieved. The reversed riser pipe, in comparison to its standard counterpart, was found to be more effective in heating water to higher temperatures. Therefore, the optimal strategy involves modifying the flat panel collector (FPC) to enhance heat transfer velocity and reduce the contact area between the fin and the riser pipe. These modifications significantly impacted the water supply temperature through the riser pipe. Karanth and Cornelio [6] embarked on a study to explore how alterations in the diameter and shape of the absorber plate conduit might impact the heat extraction capacity of the absorber plate in solar heating systems. Through computational fluid dynamics (CFD) analysis, it was discerned that tubes with a circular cross-section exhibited superior thermal performance compared to other designs. This enhanced performance, as indicated by the Nusselt number, is attributable to the optimized contact surface between the absorber plate and the tube. The study's quantitative analysis revealed significant variability in heat efficiency. The assessment of solar panel pipelines included exploring various configurations and dimensions, adhering to the criterion of maintaining uniform perimeter and cross-sectional area. The findings supported the concept that maintaining a constant cross-sectional area is pivotal, as it correlates with a notable decrease in measured pressure and a corresponding increase in absolute temperature along the length of the pipe. This research provides a compelling argument for the development of triangular pipelines in SWH systems.

Junaid et al. [7] utilized computer-aided design (CAD) software to illustrate the design of a solar flat plate collector. Employing ANSYS FLUENT 14.5 for thermal analysis and GAMBIT 2.4 for modeling, the study conducted a time-based simulation of the FPC. The analysis, carried out at specific intervals on March 11, from 11 AM to 2 PM, ensured a consistent bulk flow rate. Notably, the temperature in the collector at 12 PM was significantly higher than the initial water intake temperature of 25℃, registering at 40.89℃, thus indicating an increase of 15.890℃. A gradual decrease in temperature was observed over time. Chaudhary et al. [8] conducted a study utilizing CFD to investigate the application of solar energy in an evacuated tube heat conduit. This conduit's primary function is to convert radiation energy into thermal energy. A notable advancement in solar thermal technology is the use of nanofluids to enhance heat transmission. In this context, water and aluminium oxide (Al_2O_3) were employed as operating fluids in the heat pipelines. The study compared closed tube heat pipe (CTHP) solar water heaters with conventional evacuated tube solar water heaters, finding that the former demonstrated superior nanofluid thermal output. The research also explored how variations in the mass flow rate and the inclination angle of the condenser affect the operation of an evacuated tube heat pipe. Manilal [9] sought to enhance the numerical approach to solar collector efficiency. Their primary aim was to use numerical modelling methods to potentially increase the efficiency of solar collectors, particularly for the dehydration of livestock products. Sun drying, a viable alternative due to its economic and practical advantages, was examined through the lens of technological advancements. The study involved simulating various configurations and sizes of absorbent plates using CFD software. The goal was to surpass the efficiency levels of traditional solar collectors. A three-dimensional model of a solar flat panel collector was created using UGS NX software and saved in the STEP file format. This model was then imported into ANSYS Workbench for further simulation and analysis, with meshing carried out using ANSYS ICEM and results generated in ANSYS Fluent.

Babu et al. [10] undertook a study to assess the impact of solar water heaters on battery efficiency. In this study, the riser duct of the solar water heater was connected to an external connecting wing. A comprehensive solar accumulation analysis was then conducted using CFD methods. This approach allowed for a detailed examination of solar collectors and a more profound understanding of their heat exchange capabilities. The study juxtaposed experimental data with CFD simulations to evaluate the thermal properties of conventional SWH systems and their variants. The findings from this research indicated that the efficiency of the system could potentially be enhanced by 3-5%. This study contributes significantly to the field by providing insights into the optimization of SWH systems for improved efficiency. Despite notable advancements in SWH technologies, research gaps remain, particularly in the thermal properties of specific design systems [11]. Current studies predominantly focus on conventional designs, leaving alternative configurations such as tube over plate, tube under plate, and tube in line with plate largely unexplored. Moreover, there is a dearth of research employing the k-omega turbulence model in a systematic manner for the comprehensive assessment of the thermal performance of solar water heaters. This research posits that the k-omega turbulence model serves as an efficacious instrument for analyzing the thermal characteristics of solar water heaters. It is hypothesized that varying design configurations, namely, tube over plate, tube under plate, and tube in line with plate, will manifest distinct thermal behaviors. CFD simulations, facilitated through ANSYS software, are anticipated to yield insightful data on the thermal efficiency of each design.

The guiding research question of this investigation inquiries into the impact of different solar water heater designs on their thermal properties. Specifically, it examines how the configurations of tube over plate, tube under plate, and tube in line with plate influence thermal characteristics. Furthermore, the study explores the proficiency of the k-omega turbulence model, as implemented in CFD simulations via ANSYS software, in capturing and analyzing these thermal behaviors. A notable gap in existing research is the lack of comprehensive exploration into the thermal characteristics of solar water heaters, especially concerning varied design configurations. This gap hinders the advancement of optimized SWH systems, thereby impeding progress towards sustainable energy solutions. Therefore, the research problem is centered on the essential need for a detailed analysis of thermal behaviors within different solar water heater designs, employing the k-omega turbulence model and CFD simulations. The objective of this study is to evaluate the thermal characteristics of solar water heaters using the k-omega turbulence model. Three distinct design configurations are subjected to evaluation through CFD techniques: tube over plate, tube under plate, and tube in line with plate. The simulations are conducted using ANSYS software, aiming to provide a comprehensive understanding of the thermal dynamics involved in these systems.

2 Methodology

The methodology employed in this study involves the development of a three-dimensional CAD model of a solar water heater. This model was created using Creo Parametric design software. Key components modeled include the tube, copper plate, lower housing, upper housing, and glass plate. These individual parts were subsequently assembled to form the complete solar water-heater assembly (Figure 1).

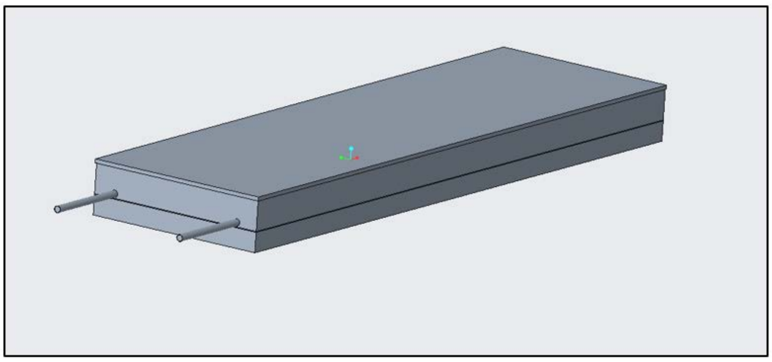

Figure 1. CAD model with a copper tube positioned underneath the copper plate

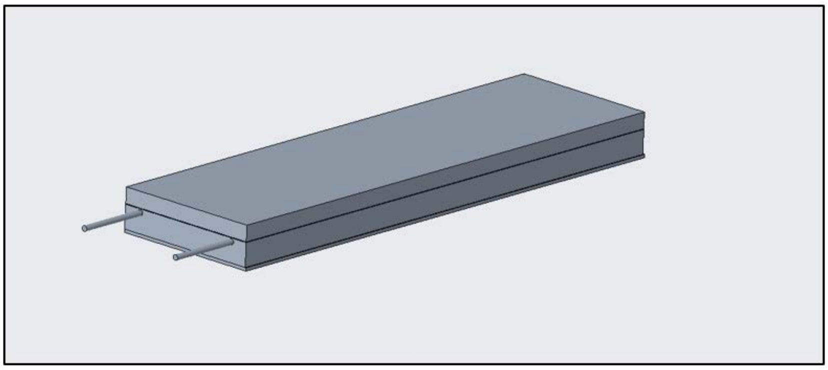

Figure 2. CAD model with the copper tube above the copper plate

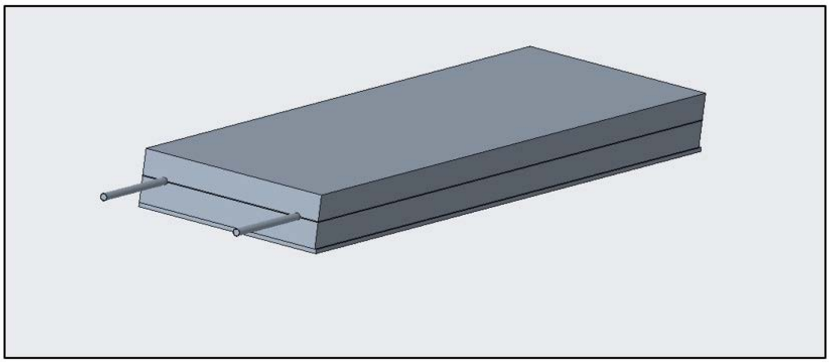

Figure 3. Copper plate leveling with the copper tubing in the CAD model

Three distinct design configurations were analyzed: tube over plate (Figure 1), tube under plate (Figure 2), and tube in-line with plate (Figure 3). The CAD model of the solar water heater was imported into the ANSYS DesignModeler module for further analysis. During the importation process, various types of imperfections, such as swivels and hard edges, were identified [11]. A comprehensive model check was conducted, and necessary corrections were applied as illustrated in Figure 4.

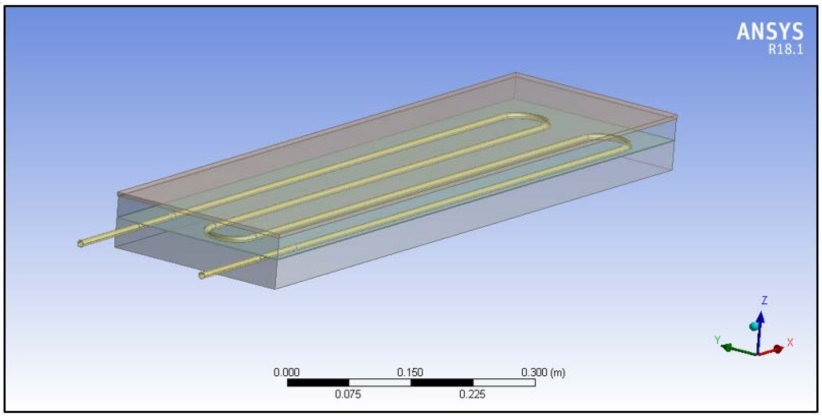

Figure 4. Corrected CAD model as imported into ANSYS Design-Modeler

To account for curvature effects within the solar water heater design, the CAD model was discretized utilizing both tetrahedral and hexahedral elements, meticulously scaled for accuracy. This process resulted in the generation of a total of 2,863,298 elements, accompanied by the creation of 773,462 nodes. The aspect ratio achieved for the tetrahedral mesh was 2, while that for the hexahedral element mesh was 1.5 as indicated in Figure 5. Additionally, the skewness for the tetrahedral element mesh was measured at 0.8, with an orthogonality of 30 degrees. For the simulation of turbulent flow conditions, the Shear Stress Transport (SST) k-omega ($k - \omega$) turbulence model was employed, classified within the Reynolds-averaged Navier-Stokes (RANS) family. This model, which encompasses all modelled turbulence effects [12, 13], operates on two key equations. It solves two transport equations, expressed as Partial Differential Equations (PDEs), alongside a storage equation. These equations incorporate historical effects, including convection and diffusion of turbulent energy. Crucial to the model are the turbulent kinetic energy (k), signifying the energy in turbulence, and the turbulent dissipation rate (ω), indicating the dissipation rate per unit of turbulent kinetic energy [14]. The k-omega model's robust performance and stability in pressure-gradient fields render it reliable for simulating complex flows in solar hydrothermal systems. Its suitability spans different flow regimes, offering improved reliability in predicting heat flux variations from laminar to turbulent solar flux.

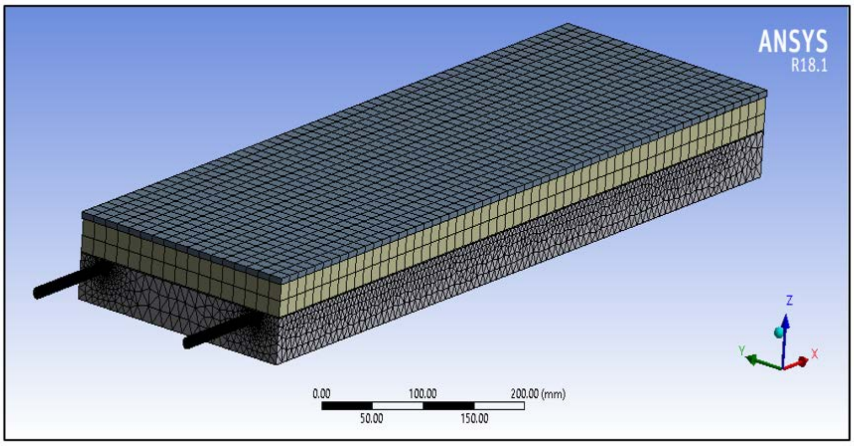

Figure 5. Mesh assembly display of the solar water heater

Distinct from other turbulence models, the SST k-omega model exhibits minimal sensitivity to free stream conditions, typically associated with flows outside the boundary layer. The shear stress limiter within the model acts as a crucial component, especially near stagnation points, preventing the excessive buildup of turbulent kinetic energy. The SST models serve as a foundational framework for further advancements, facilitating studies on the transition from laminar to turbulence and enabling the implementation of the Scale-Adaptive Simulation (SAS) technique. The boundary conditions are presented in Figure 6.

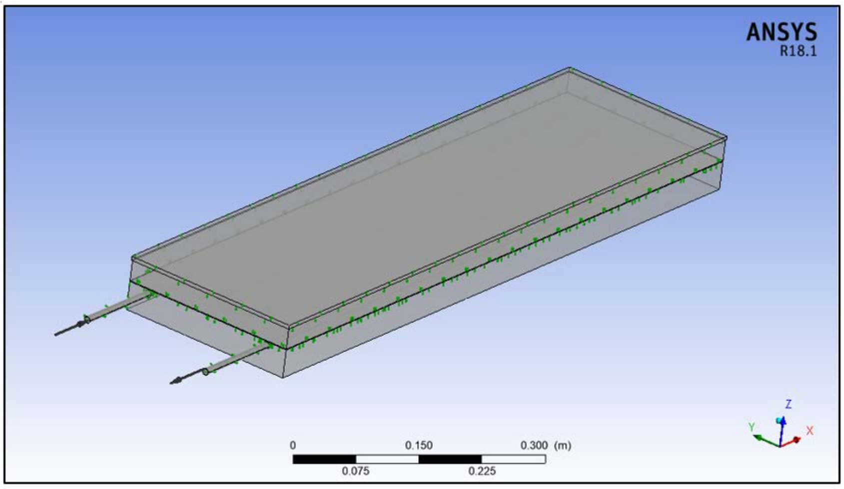

Figure 6. Representation of boundary conditions (inlet/outlet)

In the construction of the solar water-heater model, the upper portion is composed entirely of glass. Domain definitions are assigned to different zones within the model, categorized as either solid or fluid types. Specifically, the copper tube and glass components are designated as solid-type domains, as illustrated in Figure 7 and Figure 8. The upper and lower enclosures of the model are identified as fluid-type domains. The inlet of the tube is characterized by a water inlet boundary condition with a mass flow rate of 0.02 Kg/s, while the outlet is defined with a water outlet boundary condition characterized by zero relative velocity, as depicted in Figure 6. The CFD analysis is executed at two distinct time intervals: 12:30 PM and 3:30 PM. During these intervals, the heat flow values are recorded as 1040 $\mathrm{W/m^2}$ and 780 $\mathrm{W/m^2}$, respectively.

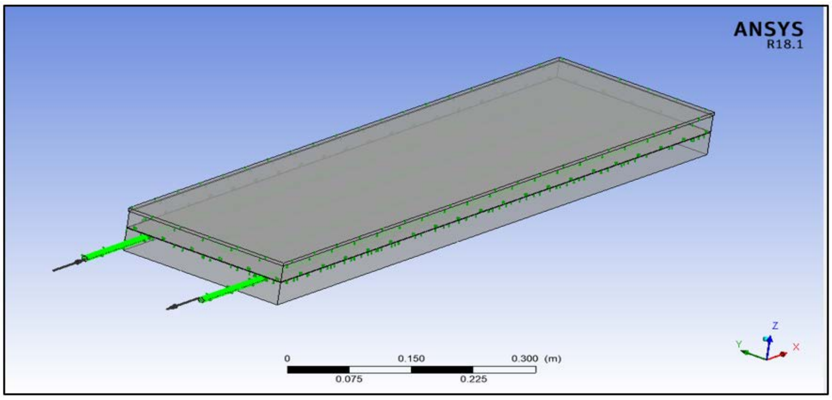

Figure 7. Copper tube domain (solid type domain)

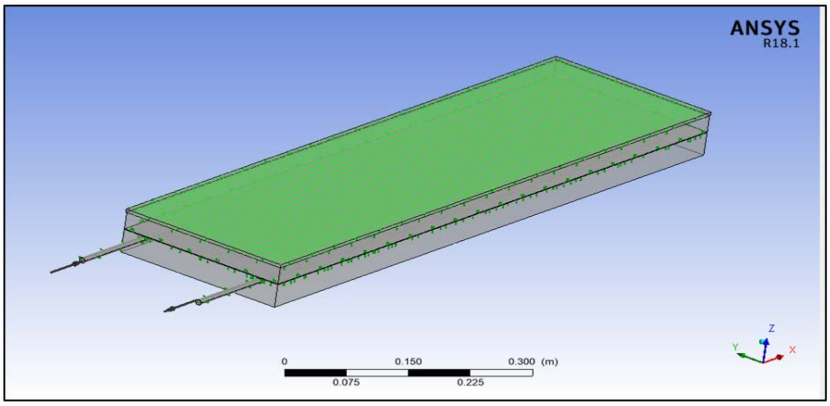

Figure 8. Glass domain (solid type domain)

In this pivotal phase of the study, the focus was on meticulously fine-tuning the solver settings within the CFD framework. This involved the precise setting of Root Mean Square (RMS) residual target values, which are essential for achieving high accuracy in the simulation of thermal characteristics of solar water heaters. The establishment of these target values marks a critical step in the quest to unravel the intricacies of thermal efficiency within these systems. Upon establishing the boundary conditions, the solver settings were carefully defined. This included the configuration of RMS residual target values for each variable under consideration, such as velocity, pressure, and temperature. In this process, the residual for each computational cell was computed as the difference between the calculated value and the value from the preceding iteration. Subsequently, the RMS residual was determined as the square root of the average of these squared residuals, taken across the total number of computational cells.

$$\text{RMS Residual } = \sqrt{\frac{1}{N}\sum_{i=1}^{N}(Residual_i)^2}$$

where, N is the total number of computational cells.

3 Results

The thermal performance of a solar water heater was evaluated through a CFD analysis using ANSYS CFX software. This investigation focused on analyzing the absorption of thermal energy and the discharge temperature under various operational conditions.

Figure 9 presents the temperature distribution within the solar water-heater operating at 780 W with a bottom plate arrangement. The highest temperature recorded in the tube, occurring at the midpoint, was 332.5K. This finding aligns closely with existing literature [15]. The temperature gradient within the solar collector showed an increase proximal to the tube, with the lowest temperature observed at the inlet. A grid independence test was conducted to ascertain the impact of mesh density on the predicted temperatures. The number of elements in the simulation grid was systematically varied from 2,863,089 to 2,863,298. Table 1 details the results of this test, demonstrating minimal temperature variation across the range of grid resolutions tested. Such consistency in temperature readings affirms the reliability of the numerical solution, indicating that the observed temperature patterns are not dependent on the mesh density. This consistency reinforces the credibility of the thermal analysis conducted.

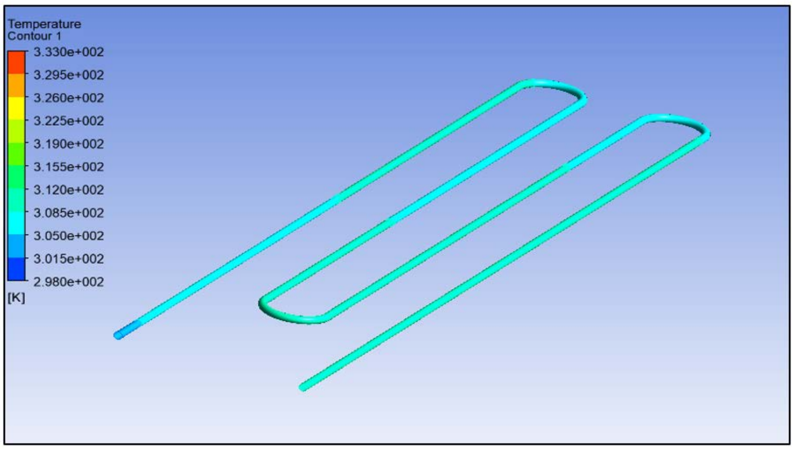

Figure 9. Temperature distribution within the solar water heater operating at 780 W with a bottom plate arrangement

Table 1. Grid independence test

Number of Elements	Temperature
2,863,089	331.89
2,863,112	331.98
2,863,191	332.41
2,863,218	332.45
2,863,298	332.50

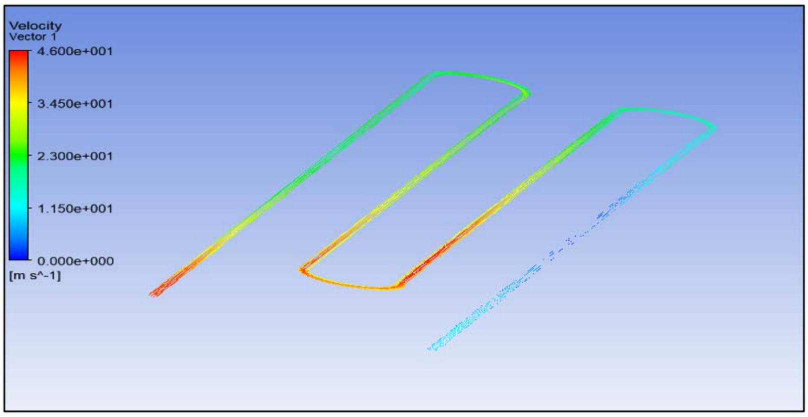

Figure 10. Velocity diagram of the solar water-heater operating at 780 W (bottom plate arrangement)

Figure 10 illustrates the velocity profile within the solar water-heater, also operating at 780 W, under a bottom plate arrangement. The velocity vector plot indicates higher velocities at the intake and the U-shaped curvature of the conduit, measuring approximately 45.5 m/s. A green color scheme in the plot signifies lower velocity magnitudes, around 22.5 m/s, at other regions within the system.

In furtherance of the thermal analysis, Figure 11 depicts the temperature distribution within the solar water-heater operating at 1040 W with a bottom plate arrangement. The peak temperature in the tube was recorded at 331.8K, particularly in the midpoint region. The temperature gradient within the collector was observed to increase in proximity to the tube, initiating from the lowest temperature at the inlet.

Figure 12 presents the velocity profile at 1040 W under the same bottom plate configuration. A red zone, indicative of elevated velocity regions, was identified in the plot. This zone, notably around the intake and the U-shaped curvature of the conduit, registered a velocity magnitude of 45.4 m/s. In contrast, the green-colored regions demonstrated velocity magnitudes not exceeding 36 m/s.

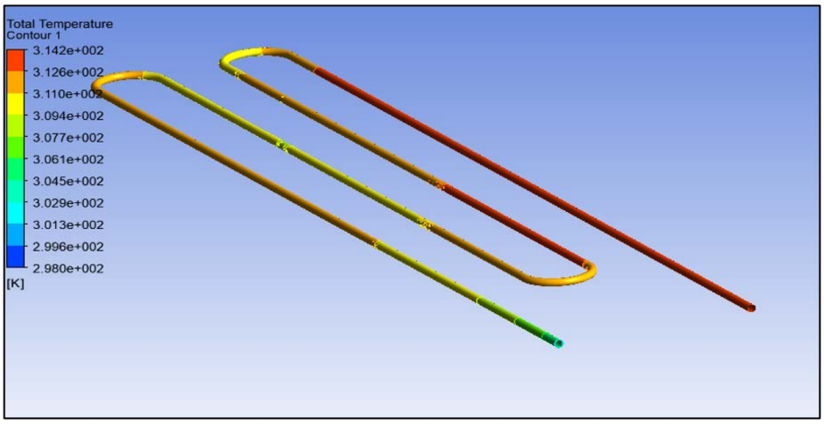

Figure 11. Temperature distribution within the solar water-heater operating at 1040 W with a bottom plate arrangement

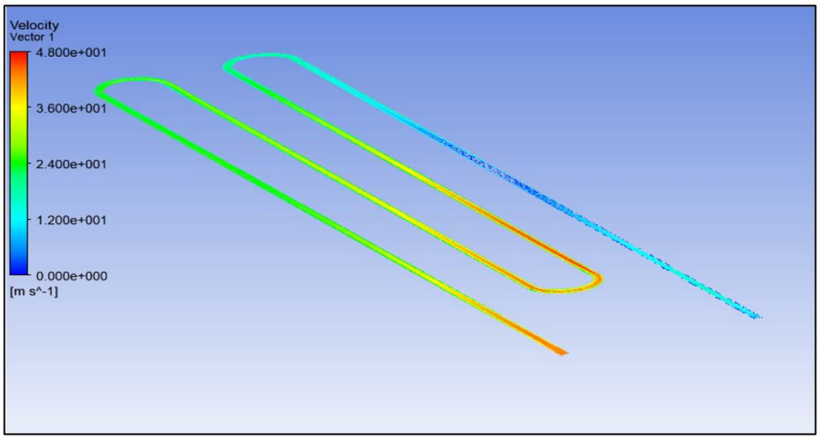

Figure 12. Velocity profile of the solar water heater at 1040 W (bottom plate configuration)

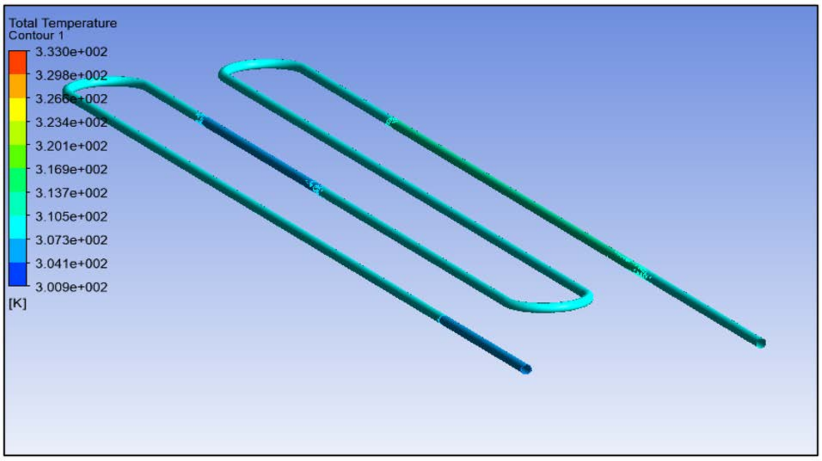

Figure 13. Temperature trend within the solar water-heater at 780 W (top plate configuration)

Turning to the top plate configuration at 780 W, Figure 13 illustrates the temperature trend within the solar water-heater. The temperature was found to be higher near the exit, following an upward trend as it approached the tube, with the lowest point at the intake.

Similarly, Figure 14 showcases the velocity plot at 780 W for the top plate configuration. The red zone, indicating higher velocities, was observed near the intake and at the U-shaped bend, reaching up to 47.6 m/s. The green zones across other areas indicated velocities approximately at 35.2 m/s.

Lastly, Figure 15 highlights the temperature plot at 1040 W for the top plate configuration. The highest temperature of the conduit was recorded at its initial point, measuring 320.2K. A consistent increase in temperature was noted towards the tube, starting from the lowest temperature at the intake.

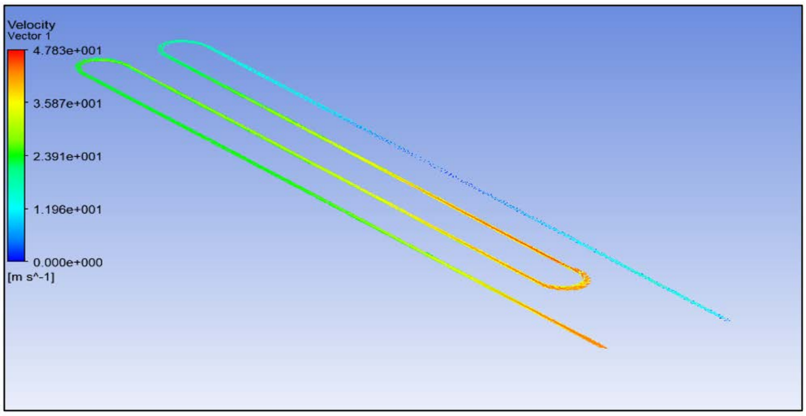

Figure 14. Velocity plot of the solar water heater at 780 W (top plate configuration)

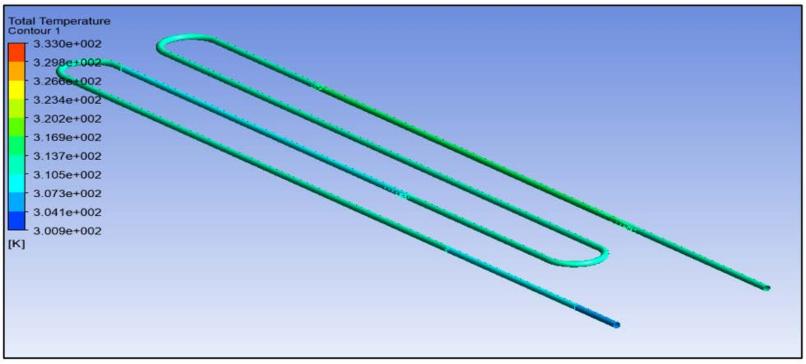

Figure 15. Temperature plot of the solar water heater at 1040 W (top plate configuration)

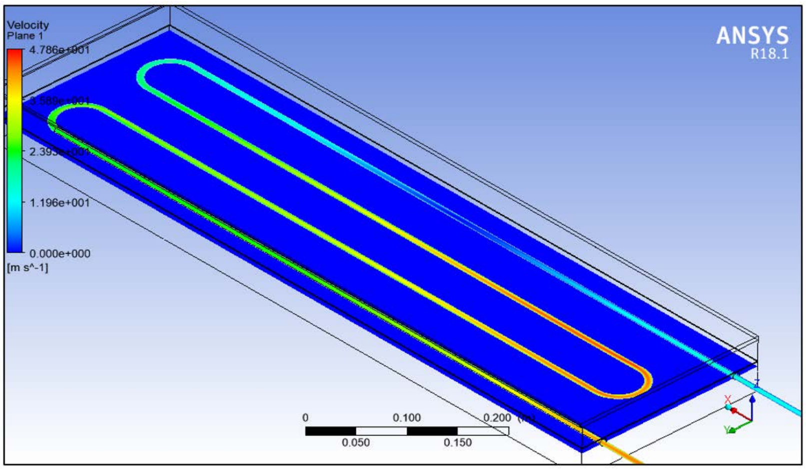

Figure 16. Velocity plot of the solar water heater at 1040 W (top plate configuration)

The velocity characteristics of the solar water-heater operating at 1040 W under a top plate configuration are elucidated in Figure 16. Elevated velocity magnitudes were recorded near the entry and at the U-shaped curve of the conduit. The red color zone in the figure indicates velocities reaching up to 46.8 m/s, while the green zones across other areas of the system show velocities around 23.2 m/s.

In Figure 17, the temperature profile for the solar water-heater at 780 W under a level plate configuration is presented. The highest temperature within the tube, observed at the output, was 321.3K. The temperature gradient within the solar collector was noted to rise as the proximity to the tube increased, with the lowest temperature registered at the inlet.

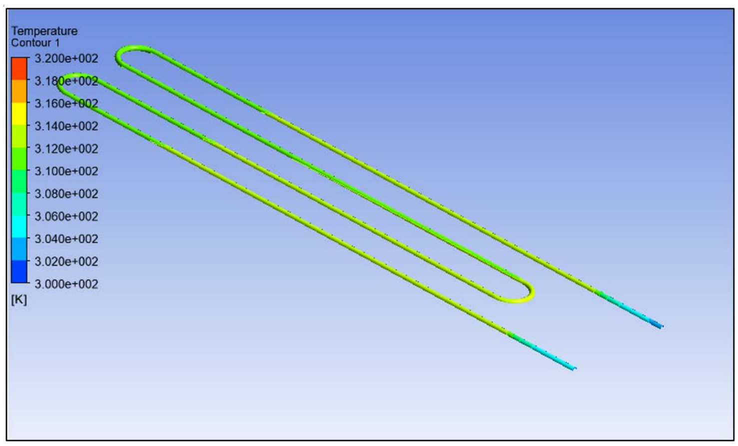

Figure 17. Temperature plot of the solar water heater at 780 W (level plate configuration)

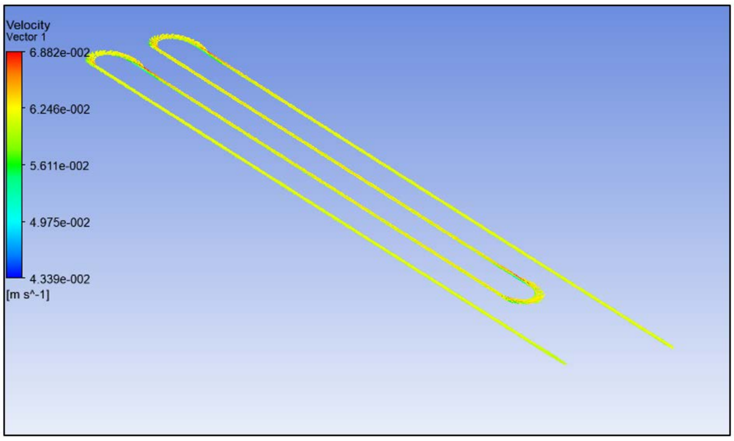

Figure 18. Velocity plot of the solar water heater at 780 W (level plate configuration)

Figure 18 displays the velocity profile of the solar water-heater at 780 W for the level plate configuration. The yellow color zone represents a steady velocity profile throughout the length of the tube, indicating a velocity value of 0.0068 m/s. This suggests a consistent and uniform flow within this particular configuration. Table 2 and Table 3, which are not included here, detail the comprehensive data for the 780W and 1040W heat flux conditions, respectively.

Table 2. Data for 780 W heat flux (12.30PM)

Design Type	$\mathbf{T_{in}}$ **(K)**	$\mathbf{T_{out}}$ **@780W**	$\mathbf{T_{780W}}$	**Heat Absorbed (J)**
Bottom plate	300	302.78	2.78	34.27
Top plate	300	303.61	3.61	41.83
Level	300	300.79	0.79	8.44

Table 3. Data for 1040 W heat flux (3.30PM)

Design Type	$\mathbf{T_{in}}$ **(K)**	$\mathbf{T_{out}}$ **@780W**	$\mathbf{T_{1040W}}$	**Heat Absorbed (J)**
Bottom plate	300	304.44	4.44	52.39
Top plate	300	304.387	4.387	51.17
Level	300	300.873	0.873	10.68

The observed temperature and velocity patterns within the solar water heater align closely with the anticipated responses, underscoring the reliability of the ANSYS CFX software. The concordance between the experimental results and established knowledge further bolsters the credibility of the findings. Figure 9, Figure 10, Figure 11, Figure 12, Figure 13, Figure 14, Figure 15, Figure 16, Figure 17, Figure 18, along with Table 2 and Table 3, provide a comprehensive and quantitative representation of these results.

This alignment not only validates the consistency and accuracy of the methodology but also highlights the potential of these findings in paving the way for future enhancements in SWH efficiency. The implications of this study extend beyond the immediate results, offering a catalyst for continued research in the domain of solar energy.

4 Conclusions

This research, utilizing CFD to explore the solar hydrothermal complex, has profoundly impacted our comprehension of thermal processes in solar water heating systems. The study not only provided insights into flow prediction but achieved this with exceptional efficiency and rapid computational timelines. A key discovery was the superior performance of plate-down tube systems, which showed close parallels with inline tube systems in terms of efficiency. Notably, the tube-below-plate configuration was identified as reaching the highest temperature, marking a peak in thermal efficiency. This apex of performance, consistently observed at 15.30 hours across all configurations, encapsulated the intricate temporal dynamics characteristic of solar water heaters.

The study's findings corroborate the initial hypothesis, affirming that the tube-below-plate configuration stands out as the most efficient design. In the pursuit of rigor and clarity, the research revisited and reinforced these results with more explicit evidence. This approach has not only validated the conclusions drawn but also underscored the reliability and significance of the data supporting these findings.

Acknowledging its scope, this study recognizes that its focus on three design configurations, while providing valuable insights, represents only an initial exploration in the vast field of solar water heater design. This acknowledgement underscores the necessity for future research to delve into more sophisticated optimization techniques. The implementation of advanced methods such as genetic algorithms (GA) and response surface methods (RSM) is suggested to further enhance the thermal performance of solar water heaters. These techniques are anticipated to unlock new dimensions in thermal efficiency, thereby refining the design and functionality of solar water heaters.

Additionally, the potential integration of parabolic reflectors in solar heating systems is proposed as a means to augment their thermal characteristics. This recommendation opens up avenues for further research, including the exploration of how these reflectors could contribute to the overall efficiency of solar water heating systems. As this study concludes, it highlights that the journey of understanding and improving the thermal dynamics of solar water heaters is far from over. The findings of this research not only contribute to the existing body of knowledge but also pave the way for future inquiries and more comprehensive explorations. The continued investigation of solar water heaters, with a focus on sustainable and optimized thermal efficiency, remains an open and inviting field of study. This research, therefore, stands as a call to action for further exploration, inspiring future advancements in the realm of solar thermal technology.

Data Availability

The data used to support the findings of this study are available from the corresponding author upon request.

Conflicts of Interest

The authors declare no conflict of interest.

References

[1] O. M. Seretse, A. Agarwal, M. T. Letsatsi, O. M. Moloko, and M. S. Batlhalefi, "Design, modelling and experimental investigation of an economic domestic STHW system using T*Sol® simulation in Botswana," in *3rd International Conference on Design, Analysis, Manufacturing and Simulation (ICDAMS 2018), Chennai, India*, vol. 172, 2018, p. 06004. https://doi.org/10.1051/matecconf/201817206004

[2] D. Prakash, "Thermal analysis of building roof assisted with water heater and insulation material," *Sādhanā*, vol. 43, no. 3, 2018. https://doi.org/10.1007/s12046-017-0781-y

[3] S. Sadhishkumar and T. Balusamy, "Thermal performance of water-in-glass evacuated tube solar collector with and without phase change material," *Indian J. Sci. Res.*, pp. 193–202, 2018.

[4] A. S. Gujrathi, S. P. Ingale, and S. U. Patil, "Analysis of parabolic trough collector using ansys fluent software," *Int. J. Creat. Res. Thoughts*, vol. 5, no. 4, pp. 2838–2843, 2017.

[5] A. K. Raj, K. Dileep, and S. Jayaraj, "Solar ETC type water heaters – An analysis based on CFD packages," *Indian J. Sci. Technol.*, vol. 10, no. 15, pp. 1–8, 2017. https://doi.org/10.17485/ijst/2017/v10i15/113827

[6] K. V. Karanth and J. A. Cornelio, "CFD analysis of a flat plate solar collector for improvement in thermal performance with geometric treatment of absorber tube," *Int. J. Appl. Eng. Res.*, vol. 12, no. 14, pp. 4415–4421, 2017.

[7] M. A. Junaid, M. Nazimuddin, M. Arifuddin, and M. Faisal, "Thermal analysis of solar flat plate collector using CFD," *Int. J. Eng. Res. Technol.*, vol. 6, pp. 659–662, 2017.

[8] Y. Chaudhary, B. Kalamkar, and P. Patel, "CFD analysis of evacuated tube heat pipe solar water heater," *Int. J. Latest Technol. Eng. Manag. Appl. Sci.*, vol. 6, no. 5, pp. 73–77, 2017.

[9] K. M. Manilal, "Design, CFD analysis and fabrication of solar flat plate collector," *Int. Res. J. Eng. Technol.*, vol. 3, no. 1, pp. 1000–1004, 2016.

[10] M. D. Babu, M. V. Ramanan, and A. Ganapathi, "Modelling and validation of solar flat plate water heating system subjected to varying absorber geometries," *Int. J. Chem. Sci.*, vol. 14, no. 4, pp. 2259–2264, 2016.

[11] A. Agarwal, O. M. Seretse, M. T. Letsatsi, L. T. Maele, and D. Koketso, "Performance evolution of an improved solar thermal hot air heating system for drying ground-nuts," *J. Mech. Eng. Res. Dev.*, vol. 42, no. 3, pp. 1–5, 2019. https://doi.org/10.26480/jmerd.03.2019.01.05

[12] A. Agarwal, M. T. Letsatsi, and I. Pitso, "Response surface optimization of heat sink used in electronic cooling applications," in *Recent Advances in Materials and Modern Manufacturing: Select Proceedings of ICAMMM 2021, Singapore*, 2022, pp. 121–129. https://doi.org/10.1007/978-981-19-0244-4_13

[13] A. Agarwal and L. Mthembu, "CFD analysis of conical diffuser under swirl flow inlet conditions using turbulence models," *Mater. Today Proc.*, vol. 27, no. 2, pp. 1350–1355, 2020. https://doi.org/10.1016/j.matpr.2020.02.621

[14] "K-Omega turbulence models," 2023. https://www.simscale.com/docs/simulation-setup/global-settings/k-omega-sst/

[15] E. Nshimyumuremyi and W. Junqi, "Thermal efficiency and cost analysis of solar water heater made in Rwanda," *Energy Explor. Exploit.*, vol. 37, no. 3, pp. 1147–1161, 2019. https://doi.org/10.1177/0144598718815240